Proceedings of the
International Conference on Mechanical Engineering and Renewable Energy 2011
(ICMERE2011) 22- 24 December 2011, Chittagong, Bangladesh

ICMERE2011-PI-171

AN EXPERIMENTAL AND COMPUTATIONAL STUDY OF A RUGBY BALL'S AERODYNAMICS

Victor Djamovski* **and Firoz Alam**

School of Aerospace, Mechanical and Manufacturing Engineering, RMIT University, Melbourne, Australia
*E-mail: s3167086@student.rmit.edu.au

Abstract- *As the Australian Rules football and the rugby ball have an odd ellipsoidal shape, they tend to differ greatly from conventional spheroid shaped sports balls in both the aerodynamic behaviour they exhibit and the axes in which they rotate. Copious amounts of data can be retrieved on spherical shaped ball; scarce information is readily available on elliptical balls on the public domain. To be able to fully grasp an understanding on these elliptical shaped balls, exhaustive experimental studies have been undertaken, for a range of varying speeds and yaw angles. The airflow around Rugby and Australian Rules foot balls was visualized and the average drag coefficients for both balls were determined and compared. The average drag coefficient for all the speeds and yaw angles was computed and compared; subsequently the corresponding Reynolds numbers variations at yaw angles were analysed; with a comparison of data analysed obtained from CFD and EFD.*

Keywords: Drag coefficient, Yaw angle, Rugby ball, Flow visualisation, Computational Fluid Dynamics (CFD), Experimental Fluid Dynamics (EFD)

1. INTRODUCTION

The aerodynamic characteristics in sports play a pivotal role in the nature of a sport balls flight properties; such as speed, spin rate decay and trajectory. Extensive research into various sports balls has been undertaken by Alam *et al.* [1-5]. Despite the popularity of sports such as Rugby, there is very little research into the aerodynamics of the game. A major part of the game of Rugby is the distance kick, be it a set shot or a drop punt during play. So with the ball travelling through the air at high speeds, crosswinds and spin play significantly on the ball's trajectory. Therefore, understanding this concept will improve the game immensely. Searching open literature for studies undertaken on the aerodynamic properties of rugby balls; with the exception of Alam et al. [2] and Seo et al. [6] it is clear that it is very hard to find any work comparing Computational Fluid Dynamics (CFD) to Experimental Fluid Dynamics (EFD). With the advent of modern computing power, CFD has become a more frequently used method of analysis. Using CFD modelling, it is easy to visualize the complex 3-dimensional flow phenomena, along with the shortened design cycles and expedient marketing. Although being time and cost effective, the CFD analysis is not a complete substitute to EFD, with both required for complete validation of data. With no follow up experiments or works of validation regarding rugby ball aerodynamics in the public domain, it seems to be the opportune time for one. Having said this, the main objective of this work was to validate the existing aerodynamic properties (being drag and side force) and juxtapose the aerodynamic properties to the CFD results. For the time being, the work has been restricted to understanding a dynamically static rugby ball; however in the near future we expect to understand the behaviour or a longitudinally rotating rugby ball.

2. EXPERIMENTAL PROCEDURE

2.1 Experimental Facilities and Equipment

The RMIT Industrial Wind Tunnel used in this study is a low-speed re- circulating wind tunnel with a six-component balance; with a maximum wind velocity of about 150 km/h with a rectangular test section measuring 3m wide, 2m high and 9m long, with turbulence level equal to approximately 1.8%. The wind tunnel is also equipped with a turntable, which enables the ball to be rotated at a desired yaw angle. A plan view of the RMIT Industrial Wind Tunnel is shown in Fig. 1. The tunnel was calibrated before conducting the experiments; with the tunnel's airspeeds being measured via a modified NPL ellipsoidal head Pitot-static tube (located at the entry of the test section) which is connected to a MKS Baratron pressure sensor through flexible tubing. The balls in focus are connected to a force sensor via a solid metal sting mount. The JR-3 force sensor is then connected to a computer, which has integrated software with an easy to use interface; allowing for

simple data retrieval of all 6 forces and moments acting on the ball (namely drag, side, and lift force, yaw, pitch and roll moments). The JR-3 force sensor used in this study, allows for a maximum measurement of 200 Newton's force, and is robust enough to carry loading. Due to its high stiffness and integration into the system, the force sensor allows minimal degradation of system dynamics, position accuracy and high resonant frequency; allowing accurate sensor response to rapid force fluctuations.

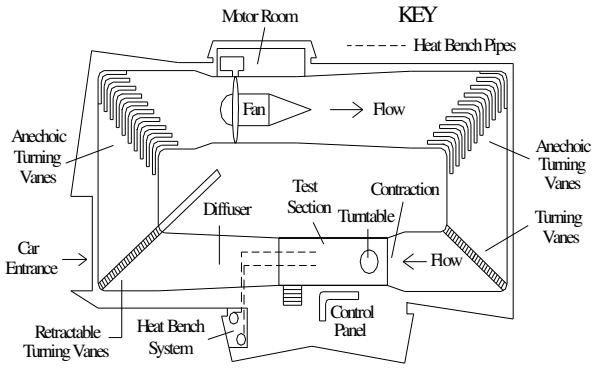

Fig. 1: Plan view of RMIT Industrial Wind Tunnel

2.2 Rugby Ball Description

A relatively old styled SUMMIT rugby ball was used, similar to that used by Alam et al. [2] being an officially licensed ball. The external measurements of the rugby ball are as follows; 280 mm long and 184 mm in diameter. The ball is made up of four synthetic rubber segments which are stitched together. The rugby ball was tested for a range of speeds (60 km/hr to 130 km/hr with increasing increments of 10 km/hr) at yaw angles varied between -90 degrees to +90 degrees with an increment of 15 degrees.

Fig. 2: Experimental set up in the RMIT Industrial Wind Tunnel with Rugby ball

Figure 2 shows the experimental set up of the rugby ball in the wind tunnels test section. The distance between the wind tunnel floor and the edge of the ball was measured to be 245 mm; which is a sufficient distance to safely ignore the ground effect as it is out of the tunnel's boundary layer. During the measurement of forces and moments, the tare forces were removed by measuring the forces on the sting mount in isolation and then removing this force from the sting and ball combination.

3. CFD MODEL AND COMPUTATIONAL PROCEDURE

A simplified version of the rugby ball was firstly designed using Solid Works; creating four smooth surfaced segments of equal dimensions. Joining the segments together created a seam structure, to replicate the real ball. The dimensions of the model are as follows; 280 mm long, 184 mm diameter and a seam indention of 2 mm, the ball can be seen in Fig. 3.

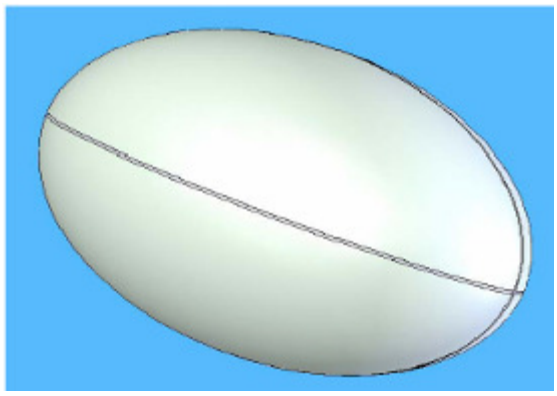

Fig. 3: Simple Solid Works model of Rugby ball

This model was then imported to GAMBIT, pre- processor of CFD code FLUENT. In CFD modelling FLUENT 6.1 was used. Within the FLUENT software, the k-ε turbulence was used. The RNG k-ε model is used in the prediction of most turbulent flow calculations because of its robustness, economy and reasonable accuracy for a wide range of flows and also suitable to rapidly straining and swirling flows. This particular turbulence model is also based on RANS (Reynolds Averaged Navier Stokes) equations.

Subsequently, a minimized model of the wind tunnel was reproduced within FLUENT; with dimensions shortened to 2500 mm in length, 2000 mm wide and 2000 mm high, saving computing time. Later, the Boolean feature within FLUENT was utilized to subtract the volume of the rugby ball from the volume of the wind tunnel. The sizing function was used to mesh the volumes; and tetrahedron grid for the rugby ball, the final mesh of the rugby ball can be seen in Figure 4.

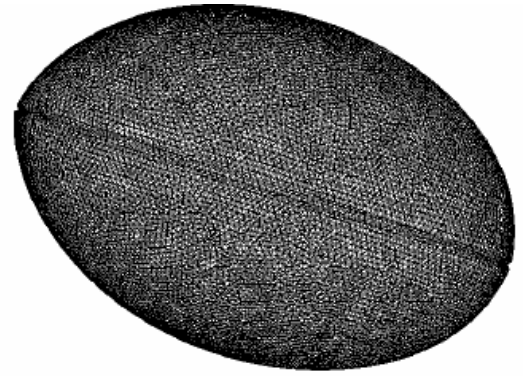

Fig. 4: Final mesh of Rugby ball

The boundary conditions of the wind tunnel were specified as follows; frontal area of wind tunnel was defined as a velocity inlet as the wind source comes from there with the rear of the wind tunnel set as a pressure outlet as the airflow exits. The rest of the boundary types were specified as walls. The boundary parameters are shown in Table 1.

Table 1: CFD modelling boundary parameters

Description	Boundary Condition
Inlet	Velocity Inlet
Outlet	Pressure Outlet
Rugby Ball	Wall
Control Volume	Wall

The accuracy of CFD solution is primarily governed by the number of cells in a grid, a larger number of cells equates to a better solution. However, an optimal solution can be achieved by using fine mesh at locations where the flow is very sensitive and relatively coarse mesh where airflow has little changes and less volatile. As mentioned earlier, Tetrahedron mesh with mid-edged nodes was used in this study. Figure 4 shows a model of the rugby ball with the tetrahedron mesh. Generally, the structured (rectangular) mesh is preferable to tetrahedron mesh as it gives more accurate results. However, there are difficulties to use structured mesh in complex geometry. Finally, the Segregated (Implicit) solver was used for the computation as it is faster and produced results close to experimental findings. Additionally, the segregated implicit solver is widely used for incompressible and mildly compressible flows. The flow was defined as in viscid, laminar and/or turbulent and as mentioned earlier, the k-epsilon model with enhanced wall treatment was used for the turbulence modelling. The non-equilibrium wall function was used as the flow is complex involving separation, re-attachment and impingement. Other model such as k-omega was also used to see the variation in solutions and results. Velocity inlet boundary conditions were used to define flow velocity and turbulence at the flow inlet. Flow inlet velocities were from 40 km/h to 140 km/h with an increment of 20 km/h at ±90° yaw angles with an increment of 30° to compare the CFD modelling results with experimental findings. The direction of airflow was normal to the inlet and the reference frame was set as absolute for the velocity. In order to control the solution, the 2nd order upwind scheme interpolation was selected as the simulation involves Tri/tetrahedral meshes. After setting all corresponding parameters, the simulation was initialized and iterated, and the results were obtained. The convergence criterion for continuity equations was set as $1x10^{-5}$ (0.001%).

4. RESULTS AND DISCUSSION

4.1 Experimental Results

The SUMMIT Rugby ball was tested at speeds ranging from 20 km/h to 130 km/h (for purposes of this paper speeds were included from 60km/h) at wind speeds under +90° to -90° yaw angles with an increment of 15° Wool tufts and smoke were utilised to help visualise the flow around the rugby ball at yaw angles 0°, 45°and 90°. The balls were yawed relative to the force sensor (which was fixed with its resolving axis along the mean flow direction whilst the ball was yawed above it) thus the wind axis system was employed. The wool tuft flow visualisation technique, for yaw angles 0° and 90° can be seen in Figures 5 and 6 respectively.

Fig. 5: Flow structure around the ball at 0° yaw angle 80km/h

Fig. 6: Flow structure round ball at 90° and 80km/h

The flow remained relatively laminar up until the middle of the 'G' on the Gilbert logo (depicted in Figure 5 with downward arrow) or around about 75-80 % from of the length of the ball from the leading edge; after which point the flow began to separate and began to chaotically re-circulate at the rear of the ball in the wake region. The averaged drag coefficient of speeds ranging from 60 km/h to 130km/h at 0° was experimentally calculated to be 0.18.

Flow visualisation was conducted at speeds of 40 and 80 km/h for the above specified yaw angles, Figure 6 represents the 80 km/h study. It is clear that for the 90° case the flow is very complex and 3 dimensional. The flow begins to separate just past the mid-way point of the top panel of the ball, whilst also being time varying. The smoke visualisation technique yielded some interested results, as can be seen in Figure 6. The flow separated began to separate between the L and B of the Gilbert emblem of the top half of the ball. At yaw angle of 90° the flow would travel from one end to the other in a swirling vortex form, and would chaotically detach and re-circulate aft of the back quarter panel of the rugby ball.

Fig. 7: Smoke visualisation at 0 degree yaw angle

Fig. 8: Flow structure round ball at 90° and 80 km/h

From Fig.8 it can be seen that there was no real Reynolds number variation present at 90°, except for the 60 and 70 km/h speeds. A certain degree of symmetry can be observed in Figure 9; indicating that the choice of placing the ball in the middle of the wind tunnel (where flow is assumed to be most uniform and developed) would show the rugby ball has been manufactured to be symmetrical down its longitudinal centreline axis. The non-dimensional parameter of drag coefficient denoted as C_D was calculated using Equation (1).

$$C_D = \frac{D}{\frac{1}{2}\rho V^2 A} \quad (1)$$

Whereby the dynamic pressure ($q=0.5\rho V^2$) was taken from the control panel of the wind tunnel, and the area was just calculated using the area of an ellipse formula.

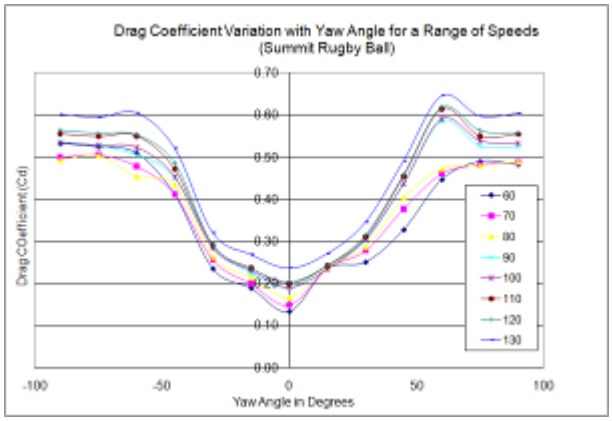

Fig. 9: Drag coefficient (C_D) as a function of yaw angle and wind speed

The side force coefficient has a minor off-set from the 0° yaw angle for the rugby ball which is believed to be attributed to a small mounting error, see Figure 9. A minor variation in Reynolds number was noticed at the lowest Reynolds number speed corresponding to 60 km/h. only a minor variation in positive and negative magnitudes of side force coefficient with changing yaw angle was noted, which again contributes to the claims that both the ball's shape and wind tunnels wind flow are not quiet symmetrical.

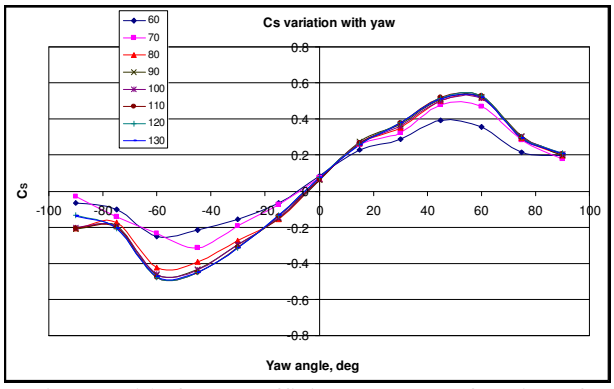

Fig. 10: Side force coefficients (Cs) as a function of yaw angles and wind speeds

4.2 Computational Fluid Dynamics Results

The CFD simulation was conducted using FLUENT 6.1 at a range of speeds (60 to 120 km/h with an increment of 20 km/h). The velocity vectors distributions around the ball at 0° and 90° yaw angles for 100 km/h can be seen in Figures 11 and 12.

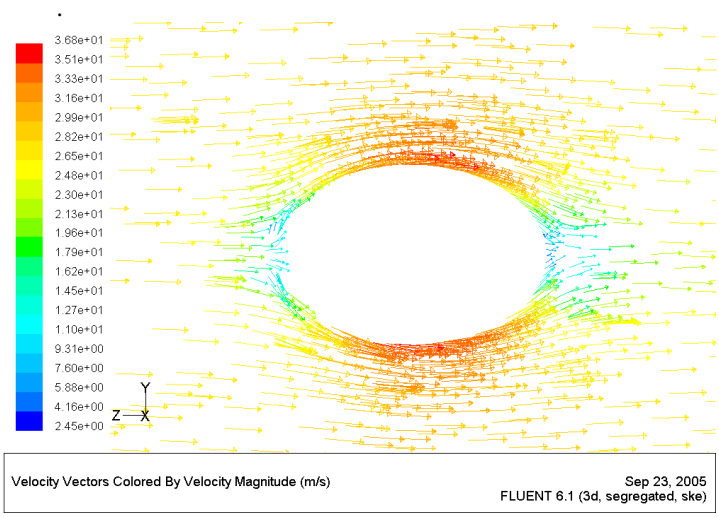

Fig. 11: Velocity vectors around the rugby ball at 0° yaw angle

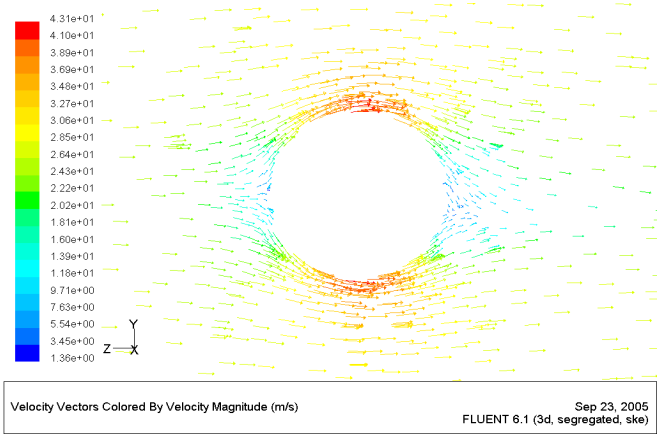

Fig. 12: Velocity vectors around the rugby ball at 90° yaw angle

Figures 11 and 12 show slight variations in the velocity vector developments between the 0° and 90° yaw angles. At 0° yaw angle, the flow remains streamlined and more of the flow is attached to the ball, compared with the 90° yaw angle. Amore chaotic velocity vector field is observed with the 90° yaw angle with the flow re-circulating at the leeward side of the ball. This observation is substantiated with the wool tuft flow visualisation of the 0° and 90°, as seen in Figures 5 to 8.

The drag coefficient and side force coefficient plots as functions of varying yaw angles and wind speeds can be viewed in Figures 13 and 14 respectively. No significant Reynolds number variation was found in CFD analysis. The drag coefficients are almost independent of Reynolds numbers. The computed minimum drag coefficient at 0º yaw angles was approximately 0.14. However, the drag coefficient increases with an increase of yaw angles (see Fig. 13). The maximum drag coefficient was found at ±90º yaw angles (approximately 0.50). No significant asymmetry of drag coefficients between the positive and negative yaw angles was noted. The side force coefficient demonstrates the highest magnitudes (0.25) at approximately ±50º yaw angles. As expected, zero side force coefficient was found at zero yaw angles.

The geometry of a real rugby ball is complex and hard to manufacture a parabolic 3D shape to perfection. However, the computational model used in this study was a perfectly symmetrical parabolic geometry, seen by the perfectly symmetrical graphs (Figures 13 and 14). Using CFD, ideal theoretical results were generated. However, both CFD and experimental results have shown similar trends. In reality, the CFD results have significant variation from experimental results. These variations are believed to be due to over simplification of the model, inability to replicate real flow around the ball, limitation of CFD software and also mirror computational and experimental errors. Using the standard approximations formula, approximate error of 1.5 % in forces coefficients was found both in experimental and computational studies, which can be considered within acceptable limits.

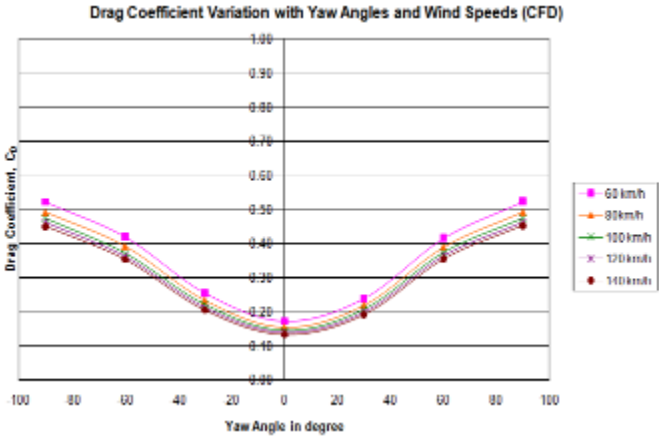

Fig. 13: CFD drag coefficient varying yaw angle and wind speed

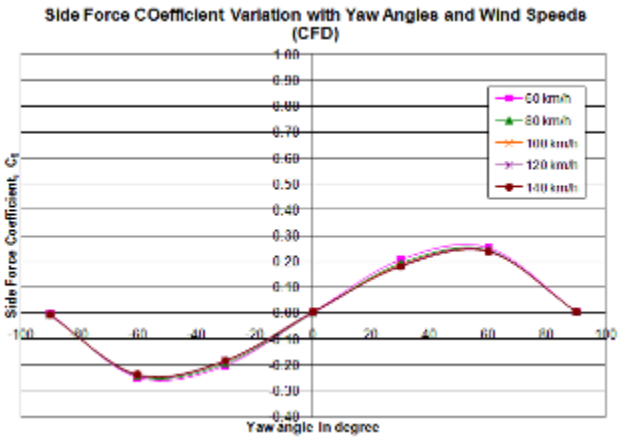

Fig. 14: CFD side force coefficient varying yaw angle and wind speed

5. CONCLUSIONS

The following conclusions can be made from the work presented here:

The aerodynamic properties of ellipsoidal shaped sports balls differs greatly from spherical shaped balls, being complex even when the ball is not spinning. The average drag coefficient for the rugby ball at 0° yaw angle was found experimentally and computationally to be 0.18 and 0.14 respectively.

The experimental and computational measurements indicated the average drag coefficient for the rugby ball at 90º yaw angles between 0.53 and 0.50 in experimental and computational studies respectively. The highest magnitude of side force coefficients for the rugby ball were found to be ±0.25 at approximately 50º yaw angles in computational modelling. However, the highest positive magnitude of side force coefficient was to be +0.53 noted at yaw angle +60° and the highest negative magnitude of -0.47 at yaw angle -60°.

Relative symmetry was found in both the drag and side force coefficient plots, showing that the ball is manufactured accordingly. No significant Reynolds number variation of drag coefficients and side force coefficients was found in computational analysis. However, some variations were noted in experimental measurements at certain yaw angles

6. ACKNOWLEDGEMENT

Sincere thanks from authors are expressed to Mr Pek Chee We and Tio Wisconsin for their extraordinary assistance with the CFD modelling.

7. REFERENCES

[1] Alam, F., Subic, A., Watkins, S. and Smits, A. J. (2010). Aerodynamics of an Australian Rules Foot Ball and Rugby Ball in *Computational Fluid Dynamics for Sport Simulation* (edited by M. Peters), ISBN 13: 978-3-642-04465-6, pp 103-127. Springer, Germany

[2] Alam, F., Subic, A., Watkins, S., Naser, J. and Rasul, M. G. (2008), "An Experimental and Computational Study of Aerodynamic Properties of Rugby Balls", WSEAS Transactions on Fluid Mechanics, Vol. 3 (3), pp 279-286, July

[3] Alam, F., Subic, A. and Watkins, S. (2005), "Measurements of aerodynamic drag forces of a rugby ball and Australian Rules football"in *The Impact of Technology on Sport I* (edited by A. Subic and S. Ujihashi), Tokyo Institute of Technology, Japan, ISBN

[4] Alam, F., We, P. C., Subic, A. and Watkins, S. (2006), "A Comparison of Aerodynamic Drag of a Rugby Ball using EFD and CFD" in *The Engineering of Sport 6* (edited by E. F. Moritz and S. Haake), Vol. 2, ISBN 0-387-34678-3, Springer Science, Munich, Germany, pp. 145-150.

[5] Alam, F., Watkins, S. and Subic, A. (2004), "The Aerodynamic Forces on a Series of Tennis Balls", *Proceedings of the 15th Australasian Fluid Mechanics Conference*, University of Sydney, 13-17 December, Sydney, Australia.

[6] Seo, K., Kobayashi, O. and Murakami, M. (2004), "Regular and irregular motion of a rugby football during flight", *The Engineering of Sport 5*, ISBN 0-9547861-0-6, pp 567-573.

[7] Asai, T., Seo, K., Kobayashi, O. and Sakashita, R. (2007) "Fundamental Aerodynamics of the Soccer Ball", ISEA Sports Engineering, Vol. 10, No.2, pp 101-109, June

[8] Mehta, R.D. and Pallis, J.M. (2001) "Sports Ball Aerodynamics: Effects of Velocity, Spin and Surface Roughness" (peer assessed) Edited by Froes, S. and Haake, S.J, Materials and Science in Sports, pp 185-197

[9] Himeno, R. (2001) "Computational Study of Influence of a Seam Line of a Ball for Baseball on Flows", Journal of Visualisation, Vol. 4, Issue 2, pp 197-207, April

[10] Alam, F., Chowdhury, H., Theppadungporn, C. and Subic, A. (2010), Measurements of aerodynamic properties of badminton shuttlecocks, Procedia Engineering, Volume 2, Issue 2, June 2010, pp 2487-2492, Elsevier, Vienna